Pure Appl. Chem., Vol. 73, No. 11, pp. 1733–1748, 2001.

Corresponding states for electrolyte solutions*

Hermann Weingärtner

Physikalische Chemie, Ruhr-Universität Bochum, D-44780 Bochum, Germany

Abstract: The equilibrium properties of electrolyte solutions over wide ranges of concentration, temperature, and solvent dielectric constant are discussed on a corresponding-states basis. If low-melting salts are used, these properties can be studied up to the pure fused salt. We mainly focus on systems at low reduced temperature, where the depth of the interaction potential is large compared with the thermal energy. Examples are singly charged ions in solvents of low dielectric constant and of highly charged ions in water. The state of the ions is discussed on the basis of thermodynamic, electrical conductance and dielectric constant data. Special attention is given to the transition to the fused salt, where ion clusters have to redissociate to form the dissociated structure of the salt. This transition can lead to liquid–liquid phase separations. The resulting critical points serve as important targets for testing theories. Examples are given for large deviations from corresponding-states behavior caused by specific short-range interactions.

INTRODUCTION

Electrolyte solutions have long been of interest to physical chemists. Our current interest focuses on wide ranges of concentration, temperature, and solvent dielectric constant, including systems completely miscible up to the fused salt. For comparing properties of ionic fluids over such wide ranges of conditions, corresponding-states correlations may be useful [1]. For a long time, corresponding-states ideas have been profitably employed for correlating the equilibrium properties of simple nonionic fluids. In the ionic case, the symmetrical charged hard-sphere fluid (the "restricted primitive model", RPM) satisfies the corresponding-states requirements as well [1]. The RPM is a reasonable model for fused salts and forms the basis of familiar solution theories such as Debye–Hückel (DH) theory and Bjerrum's theory of ion association. This success invites further study by applying the corresponding-states concept to electrolyte solutions.

We are particularly interested in states at low reduced temperature, where little is known experimentally and theoretically, and where new features such as liquid–liquid immiscibilities may occur [2,3]. For a given salt T^* is proportional to product $T{\cdot}\varepsilon$, where ε is the dielectric constant of the medium at the actual temperature T [1]. Thus, states with low T^* occur in fused salts, even if T is very high, because the medium is the vacuum with $\varepsilon = 1$ [4]. In solvents, ε is often equated with the dielectric constant ε_S of the pure solvent, so that a low reduced temperature implies a solvent of low polarity. Since for water ε_S decreases faster than T increases, high-temperature aqueous systems are also at low T^* [4,5]. The same situation applies for aqueous solutions of multivalent ions near 298 K, because T^* depends inversely on the product of the ionic charges.

At low T^*, the depth of the interionic potential is large compared with the thermal energy, so that ion pairs are formed in dilute solutions, while at higher salt concentrations, neutral and charged higher clusters may become important. At still higher concentrations, the description in terms of distinct aggre-

*Plenary lecture presented at the 27th International Conference on Solution Chemistry, Vaals, The Netherlands, 26–31 August 2001. Other presentations are published in this issue, pp. 1679–1748.

gates becomes inadequate, because the solution has to undergo a structural transition toward a fused salt. There are qualitatively new features in this transition range, including the occurrence of a liquid–liquid miscibility gap [2,3]. The resulting critical point has become an important target for testing theories, both with regard to its location in the corresponding-states diagram and to some unusual near-critical phenomena in such systems [2,4,6,7]. These new results and their interpretation constitute the primary subject of this review.

The paper is organized as follows: First, we introduce the basic features of the corresponding-states principle and discuss the choice of the corresponding-states variables. We summarize briefly the global features of the corresponding-states diagram in relation to some well-known phenomena in electrolyte solutions. The detailed discussion of these phenomena will begin with systems at intermediate reduced temperatures, $T^* = 0.10$–0.15. We will then proceed to examples at lower reduced temperatures, $T^* \cong 0.05$, where the critical point is located, and will eventually discuss cases at very low reduced temperature, $T^* \cong 0.02$, say.

While such corresponding-states correlations are quite natural for the hard-sphere ionic fluid, there is of course the question as to whether real electrolyte solutions satisfy the corresponding-states principle as well. Clearly, the interaction potentials of the RPM and of real electrolyte solutions are similar in their Coulombic part, but the presence of a solvent may introduce a wide spectrum of additional short-range interactions. In the last section of this paper, we will discuss some examples for large deviations from corresponding-states [2,3,8].

CORRESPONDING-STATES PRINCIPLE FOR IONIC FLUIDS

The requirement for corresponding-states behavior is the similarity of the interaction potential with regard to energy and distance scaling factors. The charged hard-sphere fluid satisfies these requirements [1]. In the fully symmetrical version (RPM), cations and anions with the same diameter a and with charges $q = z_+e = |z_-|e$ are immersed in a medium with dielectric constant ε. The scaling factor for the length is the hard-core diameter of the ions. The energy scale is set by the depth of the interionic potential, in the ionic case given by the Coulomb energy $q^2/(4\pi\varepsilon\varepsilon_0 a)$ at contact distance a. The reduced forms of all other parameters are then well defined, and all properties are unique functions of the reduced temperature

$$T^* = 4\,\pi\,k\,T\,\varepsilon\,\varepsilon_0\,a\,/\,q^2 \tag{1}$$

and reduced density

$$\rho^* = \rho\,a^3, \tag{2}$$

where ε_0 is the permittivity of the vacuum, and $\rho = (N_+ + N_-)/V$ is the ion density. Equation 1 implies that T^* is given by the ratio of the thermal energy kT to the depth of the interionic potential. T^* involves several factors, from which the dielectric constant can vary over a particularly wide range. ρ^* is proportional to the volume excluded by the ions. The maximum reduced density for the b.c.c. lattice is $\rho^* \cong 1.3$. We note that the now commonly used definition (2) differs by a factor of $\pi/6$ from the definition used earlier by some other authors (see, for example, ref. [1]).

Both T^* and ρ^* involve parameters which for real systems may be difficult to estimate. The space between the ions is often treated as a uniform medium with the dielectric constant of the pure solvent, but this assumption is clearly inadequate at high salt concentrations. There are also complications in estimating the diameters of large, internally flexible organic ions. Due to the cubic dependence in eq. 2, the reduced density ρ^* is very sensitive to the choice of a. Thus, mapping onto corresponding-states variables can sometimes only be done qualitatively. Table 1 quotes some figures for T^* of systems of interest later.

Table 1 Approximate reduced temperatures of typical ionic systems of interest here. Unless quoted, the temperature refers to 300 K.

T^*	System
0.60	1:1 electrolyte (a = 4.2 Å) in water
0.15	NaCl in water at 573 K
2:2	electrolyte (a = 4.2 Å) in water
	alkali halides in lower alcohols such as *n*-butanol
0.05	KI in SO_2
	tetrabutylammonium picrate in long-chain alcohols such as *n*-dodecanol
	$MgSO_4$ in water near 473 K
	NaCl at its critical point near 3200 K
0.02	tetraalkylammonium salts in apolar solvents such as CCl_4 or C_6H_{12}
	NaCl near its melting point at 1074 K

GENERAL FEATURES OF THE CORRESPONDING-STATES DIAGRAM

Figure 1 summarizes some important loci in the T^*–ρ^* diagram [1]. Due to the high dielectric constant of $\varepsilon_S \cong 80$ at room temperature, aqueous solutions of 1:1 electrolytes at room temperature are at high reduced temperatures. Except for salts with small ions, e.g., LiCl, one has $T^* \gtrsim 0.5$. Then, the depth of the interaction potential is of the order of the thermal energy, and from purely electrostatic arguments, one does not expect the occurrence of ion pairs. For example, Bjerrum's definition of ion pairs requires their interaction energy to be twice the thermal energy [9], so that ion pairs no longer exist at $T^* > 0.5$. As another feature, the high reduced temperature allows to linearize the Boltzmann factor $\exp\{-u(r)/kT\}$ of the interionic potential $u(r)$ in T^{-1}, which is a crucial ingredient of many "linear" theories such as DH theory. The range of validity of DH theory is bound to the upper left corner of the diagram. As we are mainly interested in systems at low T^*, no detailed account of behavior at high T^* will be given.

At lower T^*, where the depth of the interaction potential distinctly exceeds the thermal energy, one expects ion pairs and higher ion aggregates to become important. In this region, the mass action law for ion pair formation applies satisfactorily. Typically, the molar electrical conductance Λ decays rapidly with increasing salt concentration, because the degree of dissociation α becomes low, and for symmetrical electrolytes neutral ion pairs do not contribute to the charge transport. Bjerrum's definition of ion pairs [9] is a useful tool for describing the solution properties.

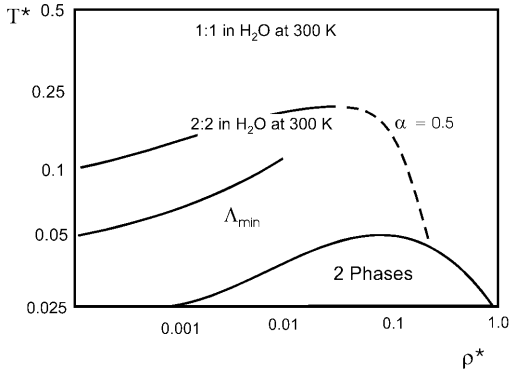

Fig. 1 Approximate corresponding-states diagram of the ionic fluid. For details, see text.

To characterize the typical range, where ion pairs dominate, we display in Fig. 1 the line corresponding to a degree of dissociation of $\alpha = 1/2$ [1]. There are two sections of this line. The solid part is calculated from strict Bjerrum theory [1]. At these ion densities, a decrease of T^* will stabilize the pairs, thus shifting the value at which $\alpha = 1/2$ to lower values of ρ^*. It is, however, obvious that this process cannot continue infinitely, because, in the end, the structural pattern of a dissociated fused salt has to be reached, although we have very low ε for the pure salt. Consequently, ion pairs will eventually disappear again, even at low T^*. This redissociation effect is particularly strong at low reduced temperatures, e.g., in apolar solvents, because a large number of pairs is formed in dilute solutions [10]. Simple Bjerrum theory does not cover these effects, and it does not make much sense to continue this line to high reduced densities. Rather, we show as a dashed line an estimated continuation based on arguments discussed later (see also ref. [11]). Clearly, this part of the line shows some ambiguity.

A consequence of this redissociation toward the fused salt is a dissociation minimum above which α increases toward higher concentrations [12]. In solvents of low dielectric constant there is indeed a minimum of the molar conductance Λ which indicates the reappearance of charged species. Following Fuoss and Kraus [13], this conductance minimum is often explained by the formation of charged ion triples. However, as expanded upon in detail below, there are several other possible mechanisms which seem more apt for explaining the redissociation toward the fused salt. Fig. 1 gives an estimate of the locus of the conductance minimum in the T^*–ρ^* plot.

Perhaps the most striking feature of the corresponding-states diagram of ionic fluids is a two-phase regime with a critical point at very low reduced temperatures. This critical point is predicted by the RPM, but for a long time its exact location was subject to debate. The best Monte–Carlo simulations currently available suggest [14]

$$T_c^* = 0.048\text{–}0.05; \qquad \rho_c^* = 0.07\text{–}0.08. \tag{3}$$

The T^*–ρ^* plot in Fig. 1 shows this coexistence curve, which in solutions should correspond to liquid–liquid coexistence [1–3]. The location of the critical point is quite distinct from that of simple neutral fluids, for example, $T_c^* = 1.31$ and $\rho^* = 0.32$ for the Lennard–Jones fluid [15].

EQUATION OF STATE AT LOW REDUCED TEMPERATURES

In following up the solution structure at low T^* over wide ranges of salt concentration, one expects several regimes of dissociation behavior. At very high dilution there are only a few ion pairs, and thermodynamic behavior should follow the well-known DH square-root laws. However, at low reduced temperatures, this regime is not reached experimentally in the range of ion densities, $\rho^* \geq 10^{-4}$ say, where experiments are feasible. Thus, one starts in the region, where the mass action law applies, and where the degree of dissociation α decreases rapidly with increasing concentration. At higher ion densities, higher charged and neutral ion clusters may occur. At still higher concentrations, the notion of pairs and higher clusters becomes inappropriate, and "redissociation" toward the fused salt structure ensues. This "redissociation" is founded in the mutual interactions between the free ions, pairs, and ion clusters. Motivated by the need for an equation of state of the RPM that accounts for observed liquid–liquid critical points, there has been much recent theoretical work on physically sound equations of state that describe this behavior and the resulting phenomena [2,6,7,16–18]. We have used some of these theories for modeling ion populations at low reduced temperatures and near critical points [19].

The basic challenge for any theory of electrolyte solutions at low T^* is the treatment of the ion configurations of high energy for which high temperature approximations commonly used in fluid-state theory, e.g., the mean spherical approximation (MSA), are inappropriate [6,7]. DH theory, for example successfully applied to dilute aqueous solutions, is a high-temperature approximation as well.

The usual way for dealing with these problems is to limit the statistical-mechanical treatment to the so-called "free" ions. Ion pairs are then taken care in a chemical model by introducing the mass action law for ion pair formation [20]

$$2\,(1-\alpha)\,/\,(\rho\,\alpha^2) = \rho_p\,/\,(\rho_+ + \rho_-) = K(T)\,(\gamma_+ + \gamma_-)\,/\,\gamma_p\,, \tag{4}$$

where α is the degree of dissociation, $K(T)$ is the pair association constant, the ρ_i are the number densities of the free ions and pairs (p), and the γ_i are the activity coefficients of the various species. Analogous extensions can be formulated for treating higher ionic clusters.

Pairing theories based on eq. 4 require the modeling of the activity. Most theories assume that ion pairs behave as thermodynamically ideal species, setting $\gamma_p = 1$. However, such an assumption is inadequate at low T^*, because ion pairs possess very large dipole moments [5,21]. For example, oppositely charged hard spheres at a distance of 4 Å have a dipole moment of about $\mu = 20$ D (1 D = $3.335 \cdot 10^{-30}$ C m). These dipolar ion pairs can interact with the free ions and with other dipolar pairs. Thus, at low T^* the picture of non interacting ion pairs cannot be retained.

If the equation of state is formulated in terms of the reduced Helmholtz free-energy density

$$\Phi = A\sigma^3/k_B TV = \Phi_{ideal} + \Phi_{excess}, \tag{5}$$

where A is the Helmholtz energy and Φ_{ideal} is the ideal gas contribution, the excess part Φ_{excess} for a system comprising free ions and dipolar pairs is of the general form

$$\Phi_{excess} = \Phi_{hc} + \Phi_{ii} + \Phi_{id} + \Phi_{di} + \Phi_{dd} - \rho_p^* \ln K(T), \tag{6}$$

where Φ_{excess} is summed over the hard-core (hc), ion–ion (ii), ion–dipole (id), dipole–ion (di), and dipole–dipole (dd) contributions. By symmetry, $\Phi_{id} = \Phi_{di}$. The last term in eq. 6 reflects the internal partition function of the ion pair, which depends on the pair equilibrium constant $K(T)$. ρ_p^* is the reduced density of the pairs. Reported equations of state for ionic fluids can be classified according to the terms retained in eq. 6 and the approximations for these terms.

$\gamma_p = 1$ implies that only the ion–ion term Φ_{ii}, with or without the hard-core term Φ_{hc}, is considered. In the last decade, several groups have attempted to derive expressions for the additional dipole and dipole–dipole interactions mainly based on DH-type approaches and on the MSA. A comprehensive review has been given recently [2]. For obtaining a simple and internally consistent treatment of the screened interactions in the complete equation of state (6) one has to resort to DH-type approaches [6], although there are many current efforts to obtain the same level for MSA-based theories [7]. One challenge for theories that incorporate dipole–dipole interactions between pairs is an adequate incorporation of a state-dependent dielectric constant, because dipole–dipole interactions between pairs cause ε to increase [15,17,22]. It was speculated a long time ago [23,24] that this increase may have distinct effects on the degree of dissociation.

Specifically, we will use the theories summarized in Table 1 for data evaluation: The first version, denoted as MSAEb, accounts for only ion–ion interactions (Φ_{ii}), and uses MSA theory to model this term. This version uses Ebeling's expression (Eb) [25] for the association constant $K(T)$ which is somewhat more accurate than Bjerrum's expression and becomes equal to it at low T^*. Thus, ion pairs are treated as thermodynamically ideal species with the activity coefficient $\gamma_p = 1$ in the mass action law. The same level of approximation is considered in terms of a DH-type theory rather than the MSA again using Ebeling's expression for the association constant (DHEb).

At a higher level of approximation a term for screened dipole–ion (DI) interactions, (Φ_{di}) between pairs and free ions is added (DHEb+DI), adopting the theory derived by Fisher and Levin [6,18]. Finally, the "complete" equation of state (6) is modeled on the basis of DH-theory by adding a term (Φ_{dd}) for screened dipole–dipole (DD) interactions between pairs (DHEb+DI+DD). This term also accounts for the state-dependence of the dielectric constant, based on a generalization of Onsager's expression for the dielectric constant of a dipolar fluid [26,27] to a system comprising free ions. This version of the theory is due to Weiss and Schröer [17].

A Carnahan–Starling form for the hard-core term (Φ_{hc}) has been applied in all calculations for obtaining consistency among the various approaches [19]. Thus, some figures differ slightly from those

reported in the original papers. Note that there are no direct MSA analogs to at the DHEb+DI and DHEb+DI+DD levels. Some more approximate treatments based on the MSA are discussed in ref. [2].

Table 2 summarizes the predictions of these theories for some distinct points in the corresponding-states diagram [19]: the critical temperature (T_c*), the critical density (ρ_c*), the degree of dissociation at the critical point (α_c), the location of the dissociation minimum at the critical temperature (ρ^*_{min}), the degree of dissociation at this minimum (α_{min}), and the upper temperature T_u* at which the locus of the minima of α terminates.

Table 2 Distinct points in the corresponding-states diagram according to various approximations used for eq. 6 [19].

Theory	T_c*	ρ_c*	α_c	ρ^*_{min}	α_{min}	T_u*
MSAEb	0.0788	0.026			0.154	
DHEb	0.0615	0.052	0.083	0.012	0.012	0.121
DHEb+DI	0.0521	0.024	0.144	0.0019	0.0049	0.115
DHEb+DI+DD	0.0548	0.0076	0.517	0.00040	0.0158	0.400

AQUEOUS SOLUTIONS OF 2:2 ELECTROLYTES

An important group of partially associated systems are aqueous solutions of 2:2 electrolytes such as $MgSO_4$ or $ZnSO_4$. With a = 4.2 Å one finds at 298 K T^* = 0.15 (*cf.*, Table 1). The speciation in such systems is well investigated theoretically [1], including solutions which are sufficiently concentrated that redissociation ensues [28]. Figure 1 shows that in concentrated solutions one should just cross the α = 1/2 line, but then redissociation drives the α = 1/2 line toward lower T^*. Thus, one expects that the degree of dissociation does not exceed markedly a value of α = 0.5, even at very high salt concentrations. Results of a cluster theory of electrolytes applied to aqueous $MgSO_4$ at 373 K [28] support this view.

In the absence of simple conductance theories for high concentrations, one may resort to the conductance-viscosity (or "Walden") product as a measure for the apparent degree of dissociation

$$\alpha_{app} = \Lambda\eta / (\Lambda_0\eta_0), \tag{7}$$

where η is the viscosity of the solution and subscript "0" refers to infinite dilution of the ions. In a study of transport processes in concentrated aqueous solutions of $ZnSO_4$ [29] we have determined the isotherm for α_{app} at 298 K. Figure 2 indicates a minimum of α_{app} near a molar concentration of $C \cong 0.5$ mol dm^{-3} ($\rho^* \cong 0.045$). Obviously suppressed by the increasing solution viscosity, Λ itself does not show a minimum.

An increase of the temperature will decrease T^*, because of the strong decrease of ε_S of water. As an interesting feature of 2:2 electrolyte behavior, one then reaches the region, where two-phase coexistence is found (*cf.*, Fig. 1). Thus, one expects liquid–liquid phase separation in aqueous solutions of 2:2 electrolytes at high temperature, typically above 473 K [30]. Thereby, the upper critical point of the RPM turns into a lower critical point in the real system, because the product $\varepsilon_S \cdot T$ decreases.

In general, 2:2-electrolytes that are highly soluble near room temperature become practically insoluble at high temperatures. For aqueous $MgSO_4$, this retrograde behavior of the solubility sets in near 340 K. Figure 3 shows the behavior of the crystallization curve as a function of the molal concentration m of the salt. However, up to this melting curve the major thermodynamic functions of $MgSO_4$ are characterized well enough to perform an extrapolation into the metastable regime. This extrapolation predicts a violation of thermodynamic stability not far above the crystallization curve [30], and by superheating we have indeed observed fluctuations near 470 K that are indicative for liquid–liquid phase separation before crystallization sets in [31]. The extrapolated metastable liquid–liquid coexis-

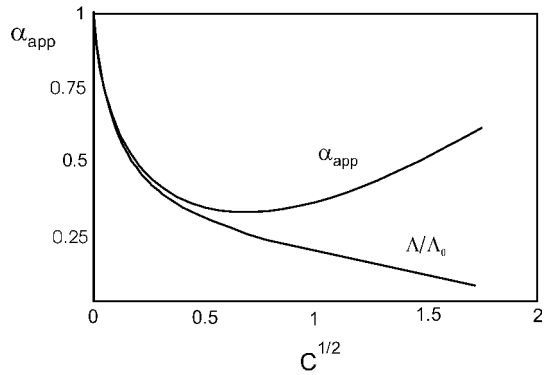

Fig. 2 Apparent degree of dissociation in aqueous solutions of $ZnSO_4$ at 298.15 K derived from the conductance viscosity product. The behavior of the molar conductance is also indicated.

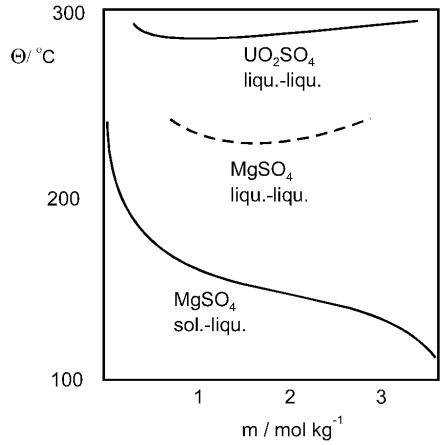

Fig. 3 Metastable liquid–liquid coexistence for $MgSO_4$ extrapolated from thermodynamic data in the liquid range in relation to the crystallization curve. The stable miscibility gap of UO_2SO_4 is also shown.

tence curve shown in Fig. 3 should be fairly typical for aqueous solutions of sulfates with bivalent cations. For UO_2SO_4, a stable miscibility gap is observed above 560 K [32] (*cf.,* Fig. 3), but UO_2SO_4 behaves more complex than simple ionic UO_2^{2+} SO_4^{2-}. There are examples for other salts with multivalent ions that show metastable or even stable liquid–liquid phase separations in water at high temperatures [33]. A prominent example is $BaCl_2 + H_2O$ [34].

ORIGIN OF THE CONDUCTANCE MINIMUM IN SOLVENTS OF LOW POLARITY

At lower reduced temperatures the minimum degree of dissociation is displaced to lower ion densities (*cf.,* Fig. 1). If at lower concentrations mobility effects associated with the viscosity are less stringent, the molar conductance Λ itself exhibits a minimum. Such conductance minima have been observed in numerous conductance studies for 1:1 electrolytes in solvents of low and intermediate polarity. Over the years, their origin has been the subject of controversial debate.

Typical examples for $T^* \cong 0.10$ are solutions of tetraalkylammonium salts in dichloromethane (CH_2Cl_2, $\varepsilon_S = 9.1$) at 298 K [5]. According to the work of Songstad and collaborators [35–37], this is just the regime where, depending on the ion sizes, the conductance minimum begins to develop. In an

attempt to reassess such data in the light of the more recent theoretical developments, we have reconsidered some of these systems.

Figure 4 shows the concentration dependence of the molar conductance and dielectric constant of tetra-*n*-butylammonium iodide (Bu_4NI) in CH_2Cl_2) [5,38]. From the low-concentration data of Songstad *et al*. [35] we find $\Lambda_0 = 108$ S cm^2 mol^{-1} and $K \cong 2 \cdot 10^4$ dm^3 mol^{-1}. Λ decreases from infinite dilution up to the minimum near $C = 0.025$ mol dm^{-3} ($\rho^* \cong 0.0065$) by about a factor of 10. Irrespective of some uncertainty in the hard sphere diameter, the low-concentration behavior is fairly consistent with the Bjerrum prediction.

Dipolar ion pairs reflect themselves in dielectric relaxation spectroscopy. As the solutions are conducting, the determination of the static dielectric constant ε requires the measurement of the frequency-dependent complex permittivity $\varepsilon^*(\omega)$. ε is defined as the zero-frequency limit of the real part of $\varepsilon^*(\omega)$, obtained through data fitting and zero-frequency extrapolation. Because the spectra reflect two modes caused by the reorientation of solvent dipoles and ion pair dipoles, such measurements can also be used to separate in a straightforward manner the static dielectric constant into an ion pair and solvent contribution [5,37].

For Bu_4NI in CH_2Cl_2 [5,38] this separation is shown in Fig. 4. The static dielectric constant increases largely with increasing salt concentration. As shown below, this increase of ε may form an essential ingredient for understanding the solution properties. The increase results solely from the ion pair contribution. The slight decrease of the solvent contribution is readily explained by the decrease in the number of solvent molecules per volume. The trends observed here are largely enhanced at lower reduced temperatures, i.e., in solvents of lower dielectric constant. We will therefore postpone a more detailed discussion of dielectric behavior until solutions at low T^* are considered.

The interesting question is what causes the reappearance of charged species at higher concentrations. The traditional explanation goes back to the work of Fuoss and Kraus [13] which ascribes the minimum to the formation of charged triple ions according to the mass action equilibria $M^+ + MX \rightleftarrows M_2X^+$ and $X^- + MX \rightleftarrows MX_2^-$. This hypothesis has become so popular that conductance minima are often considered as a definite proof of the triple ion concept. On general grounds, a high stability of triple ions can, however, be doubted [18], and, over the years, there have been alternative explanations. In particular, Kraus himself seems to have rejected the triple ion concept in later work in favor of a redissociation approach in which ion pairs decay to free ions due to the action of the fields of other free ions [10,39]. In the same spirit, Sukhotin and Timofeeva [40] have explained the conductance minimum by the breakup of pairs due to increased Debye shielding of the free ions. In both cases, a correct treat-

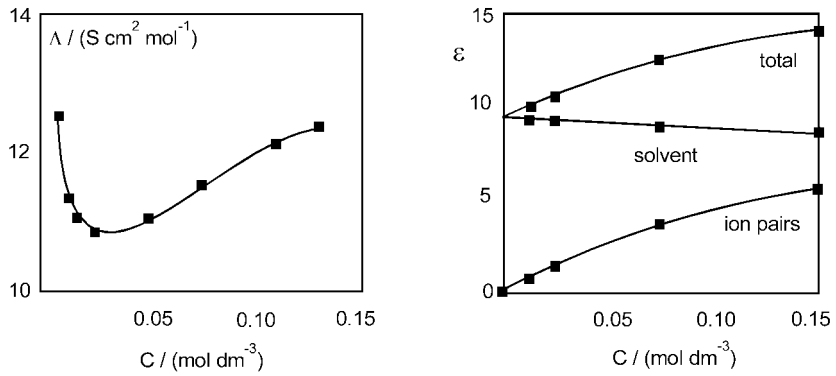

Fig. 4 Concentration dependence of the electrical conductance and static dielectric constant of solutions of tetra-*n*-butylammonium iodide in dichoromethane near the conductance minimum.

ment of the activity coefficients of the free ions in the mass action law should reveal the observed behavior, because the model implies that redissociation is already founded in the Φ_{ii} term. In contrast, Cavell and Knight [24] have argued that the increase of the dielectric constant by the increasing number of ion pairs leads to an increase of the static dielectric constant which, in turn, decreases the association constant. In terms of eq. 6 the latter argument attributes the essential mechanism of redissociation to the Φ_{dd} term for ion pair–ion pair interactions.

We consider in Fig. 5 predictions of the DH-based models in this regime, specifically at $T^* = 0.08$ [19]. All approximations reproduce the minimum of α. In particular, one finds an association minimum in the DHEb version, which indicates that even in a simple mass action treatment with $\gamma_p = 1$ triple ions have not necessarily to be invoked for explaining conductance minima, provided that the activity coefficients of the free ions are taken into account in a correct manner. Almost two decades ago, Ebeling and Grigo [41] have pointed out this aspect, when modeling the conductance on the basis of a MSAEb approach. The results of the more elaborate DHEb+DI and DHEb+DI+DD models further confirm that the existence of triple ions is not a prerequisite for explaining the conductance minimum.

While at $T^* = 0.08$ the various versions agree in the global behavior, major differences become obvious, when considering dissociation over larger ranges of reduced temperature. Figure 6 shows the loci of the minima of α in the T^*–ρ^* plot according to the various approaches [19]. Experimentally, one finds that a decrease of T^*, for example, by decreasing the static dielectric constant of the solvent, shifts the minimum to lower ion densities. Eventually, at very low T^*, e.g., in solutions in benzene [10,12,39]

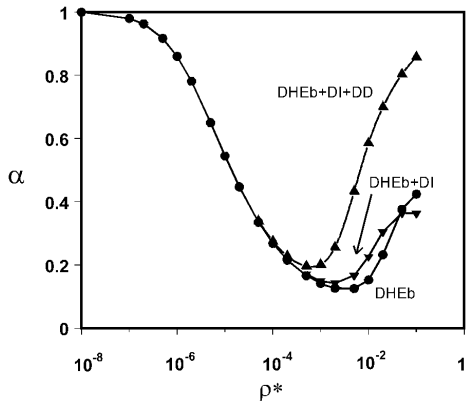

Fig. 5 Isotherms of the degree of dissociation predicted by various theories at $T^* = 0.08$.

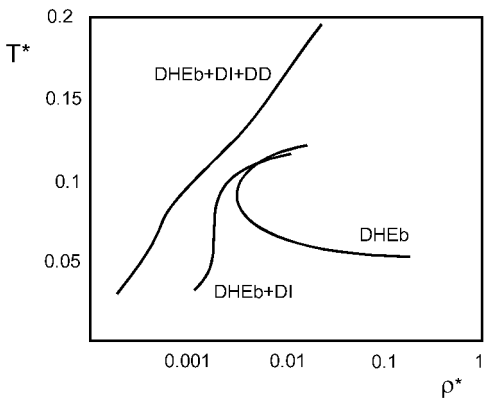

Fig. 6 Locus of conductance minima according to various models.

or CCl_4 [21], only the increasing branch of Λ can be observed in the experimentally accessible range at $\rho^* \gtrsim 10^{-4}$.

All theories examined by us predict an upper limiting temperature T_u^*, above which the dissociation minimum disappears (*cf.*, last column in Table 2). Only in the DHEb+DI+DD version this minimum is distinctly above $T^* = 0.15$ and, upon detailed inspection [19], it results from the increase of the dielectric constant by the increasing number of ion pairs. The dipole–dipole interactions themselves stabilize the pairs [19]. The fact that all theories neglecting DD interactions locate T_u^* at unreasonably low temperatures seems to indicate that the increase of ε by the increasing number of ion pairs plays an important role in the redissociation process. However, as a common feature becoming more obvious below, all approximations overestimate the degree of dissociation with regard to experimental data and to results from Monte–Carlo simulations of the RPM [2,17,19]. Note that experimentalists have discussed many rules of thumb for shift of the minimum, e.g., assuming $C^{1/3} \propto 1/\varepsilon_S$, which in terms of our formulation implies $T^* \propto \rho^{*1/3}$. None of the known rules is supported by our model calculations.

Furthermore, Fig. 6 shows that only DHEb+DI+DD theory provides a smooth behavior. DHEb becomes unphysical at $T^* < 0.08$, where the minimum begins to shift to higher temperatures and finally even disappears near $T^* = 0.05$. The DHEb+DI version is still reminiscent of this behavior, in showing an S-shaped curve in this regime. Again, it seems that the proper inclusion of DD interactions between ion pairs and an account for the increase in the dielectric constant is vital. On the other hand, in DHEb+DI+DD theory the minima are located at too low concentrations, i.e., ionicity is largely overestimated.

In conclusion, it seems fair to say that there lacks still a quantitatively accurate theory of the conductance minimum. However, a good qualitative picture has evolved. There is no need for invoking triple ions. The shielding of pairs by the free ions can already cause the conductance to increase, but this simple picture fails at lower T^*, where DI and DD interactions become increasingly important. In particular, the increase of the dielectric constant by the increasing number of ion pairs seems to form an important ingredient.

LIQUID–LIQUID IMMISCIBILITIES AND CRITICAL POINTS

As another major feature, the RPM possesses a two-phase regime with an upper critical point at $T^* \cong 0.05$. By corresponding-states arguments, one predicts this two-phase regime to correspond to a liquid–liquid critical point of 1:1 electrolytes near room temperature in solvents with $\varepsilon_S \cong 5$. If solubility permits, and if specific interactions that enhance miscibility are absent, one indeed observes immiscibilities quite similar in location and shape to the RPM coexistence curve in Fig. 1 [3]. In some cases, the critical points are located sufficiently close to room temperature to enable accurate studies of near-critical behavior, which for nonionic fluids is known to be nonanalytical. We will not consider here the near-critical behavior of ionic fluids, but we note that there are some fascinating problems with regard to the effect of the screened Coulombic interactions upon the near-critical properties that can be experimentally studied at liquid–liquid critical points. For a comprehensive review of the latter subject, we refer to ref. [2].

Until some time ago, only few ionic systems with such liquid–liquid unmixing were known [23], and there were complications in all cases that rendered proper interpretation difficult. If solidification is suppressed, e.g., in systems comprising low-melting salts [3,42], liquid–liquid miscibility gaps can readily be observed for many systems. It has already been noted that, if ε_S decreases faster than T increases, the upper critical point of the RPM corresponds to a lower consolute point in the real system. Systems of this type are known [43,44], including the stable [32] and metastable [30] miscibility gaps of 2:2 electrolytes in water at high temperatures mentioned earlier.

Instructive examples for near-critical systems are solutions of tetraalkylammonium picrates dissolved in homologous alcohols [3,42]. Much can be learned by studying the shift of the critical point

along the homologous solvent series. Figure 7 shows the product $\varepsilon_S \cdot T_c$ for one of these salts, tetra-*n*-butylammonium picrate (Bu_4NPic), as a function of the chain length n of the alkyl residues in normal and branched alcohols [2,42]. ε_S ranges from 16.8 to 3.8. If the charge q and the diameter a are fixed, the product $\varepsilon_S \cdot T_c$ should be constant, we estimate $\varepsilon_S \cdot T_c \cong 800 - 1000$ for Bu_4NPic. Figure 7 clearly shows that when increasing the apolar part of the solvent molecules, one approaches this "Coulombic limit". However, for systems containing lower alcohols, specific short-range interactions have a large effect upon the location of the critical point. Obviously, the critical point can serve as a sensitive target for studying the role of Coulombic vs. non-Coulombic contributions to the potential [8].

To elucidate the forces driving criticality, Table 2 compiles results for the critical parameters of various theories. In all cases, the critical temperature is fairly well reproduced both with regard to experimental estimates [3] and Monte–Carlo simulations [14]. However, the critical densities are underestimated. Experimentally, one finds a broad band of critical densities, but there is reason to believe that in cases where Coulombic interactions dominate one typically has $\rho^* \gtrsim 0.1$ [3,8].

At a first glance at the figures in Table 2, DHEb theory gives the best prediction of the critical density. However, this result is fortuitous, because the coexistence curve of this version (not shown here) has a physically unreasonable "buttonhole" form [16,19], which narrows at lower concentrations and terminates near $T^* = 0.051$ in a lower consolute point. This unreasonable behavior is closely related to the unphysical behavior of α_{min} in Fig. 6. From the remaining approaches the DHEb+DI theory gives better results than DHEb+DI+DD version. The better performance of the less-complete DHEb+DI theory makes one suspicious that its success is to some degree fortuitous [16,17].

Some insight into this problem comes from a more detailed consideration of the forces driving criticality. To assess these forces, a characterization of the species distribution and degree of dissociation in concentrated solutions is crucial. If one experimentally determines the conductance along the critical isotherm, one finds that the critical point is located well above the conductance minimum [3]. Thus, also from this point of view effects beyond simple Bjerrum pairing must participate in driving the phase separation. Unfortunately, the absolute determination of α_c is somewhat ambiguous, because eq. 7 is only a rough approximation. Based on the Walden products we find at criticality = 0.02–0.05 [5]. This is distinctly lower than the theoretical figures in Table 2, particularly at the DHEb+DI+DD level. It can be shown [19] that the predicted high ionicities reflect the same deficit as the underestimated critical density.

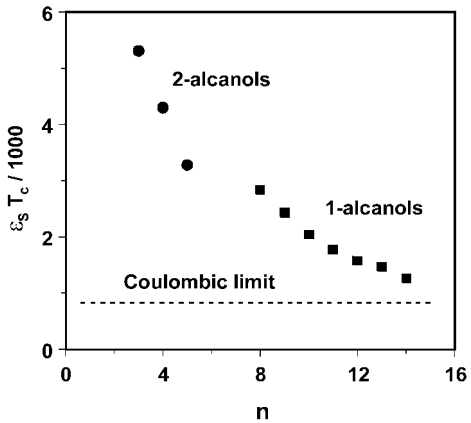

Fig. 7 Dielectric constant-temperature product of tetra-*n*-butylammonium picrate in homologous alcohols at the critical temperature.

DIELECTRIC BEHAVIOR AT LOW REDUCED TEMPERATURES

One of the keys issues in developing a more accurate equation of state is obviously a better understanding of dielectric behavior, which may benefit largely from approaches used in work on nonionic liquids. To follow this path, we first consider Onsager's theory of the dielectric constant, because this is the level at which Weiss and Schröer have built in a state-dependent dielectric constant into the expression for free energy [17]. Onsager considers a molecule with dipole moment μ, embedded in a continuum with the macroscopic dielectric constant of the substance [26,27]. It is tempting to use this approach for treating DD interactions in electrolyte solutions [16], but detailed inspection shows that the application of Onsager theory to conducting fluids needs modification, because the free ions screen the DD interactions. This screening reduces the contribution of DD interactions to the free energy, and reduces the dielectric constant with respect to its value for the purely dipolar fluid. Weiss and Schröer [17] correct for this screening by a factor g_{ion}, which depends on the Debye screening length κ of the system. For a solution comprising ion pairs of number density ρ_{p} with dipole moment μ_{p}, the modified Onsager expression reads

$$g_{\mathrm{ion}}(\kappa)\, \rho_{\mathrm{p}}\, {\mu_{\mathrm{p}}}^2 = (9\, k\, T / 4\pi)\, (\varepsilon - \varepsilon_\infty)\, (2\varepsilon + \varepsilon_\infty) / [\varepsilon\, (\varepsilon_\infty + 2)^2], \tag{8}$$

where $\varepsilon_\infty \cong n^2$ is the high-frequency limit of the dielectric constant, approximately given by the square of the refractive index. Detailed expression for $g_{\mathrm{ion}}(\kappa)$ may be found in refs. [17] and [22]. For $g_{\mathrm{ion}}(\kappa) = 1$ the Onsager expression for a purely dipolar fluid is recovered. We were suspicious [21,45] that an insufficient treatment of dielectric behavior is founded in the use of a theory at the Onsager level.

A glance at work on dielectric studies of nonelectrolyte fluids immediately shows the deficit of the Onsager approach. For particles with high dipole moment one expects orientational correlations between neighboring dipoles. Clearly, such a situation is encountered in solutions containing ion pairs with high dipole moments. For a purely dipolar fluid, Kirkwood and Fröhlich have derived a correction factor for these correlations, the well-known Kirkwood correlation factor g. Values of $g > 1$ imply preferred parallel configurations of the dipoles, $g < 1$ signals antiparallel configurations. When neglecting the correlations ($g = 1$), one recovers the Onsager expression. An extension to systems comprising free ions has been derived recently. The modified Kirkwood–Fröhlich expression for the static dielectric constant of a conducting system reads [22]

$$g\, g_{\mathrm{ion}}(\kappa)\, \rho_{\mathrm{p}}\, {\mu_{\mathrm{p}}}^2 = (9\, k\, T / 4\pi)\, (\varepsilon - \varepsilon_\infty)\, (2\varepsilon + \varepsilon_\infty) / [\varepsilon\, (\varepsilon_\infty + 2)^2], \tag{9}$$

with the same screening factor $g_{\mathrm{ion}}(\kappa)$ as in eq. 8. For $g_{\mathrm{ion}}(\kappa) = 1$ one recovers the Kirkwood–Fröhlich expression for the purely dipolar fluid.

One can now try to analyze the left hand site of eq. 9 from the dielectric data in conjunction with electrical conductance data. In practice, one may go the following way: one estimates the ion pair and free ion concentrations from the mass action law. The free ion concentration is then used to calculate the Debye screening length, and thus the correction factor $g_{\mathrm{ion}}(\kappa)$. Finally, the dipole moment of the isolated molecule is determined by extrapolation, forcing the correlation factor g to approach unity at $\rho_{\mathrm{p}} = 0$.

Figure 8 shows preliminary results for tetrabutylammonium bromide (Bu_4NBr) in chloroform ($CHCl_3$) [31] and in tetrachloromethane (CCl_4) [21]. $CHCl_3$ has $\varepsilon = 5.1$, and T^* is slightly above the critical temperature of the RPM. CCl_4 has $\varepsilon_{\mathrm{S}} = 2.23$, thus $T^* \cong 0.025$, which corresponds to conditions at the lower part of the theoretical miscibility gap. Surprisingly, there is however complete miscibility, clearly indicating a major role of non-Coulombic forces in determining the equilibrium properties. Nevertheless, this system should yield important information on dielectric behavior at low T^*. We note that in CCl_4 the conductance minimum is obviously shifted to such low concentrations that in the accessible range one observes only the branch, where Λ increases with increasing salt concentration. Hence, the free ion concentration is so low at the concentrations of interest that data evaluation neglecting the

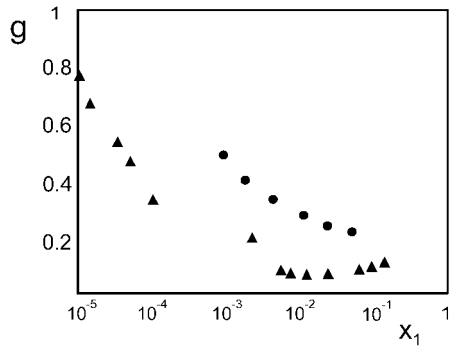

Fig. 8 Kirkwood factor g for ion pair correlations of solutions of tetra-*n*-butylammonium bromide in carbon tetrachloride (circles) and chloroform (triangles). x_1 is the mole fraction of the salt.

free ions and their screening is sufficient. Thus, one practically applies the pure Kirkwood–Fröhlich theory.

It is seen that $g < 1$ in all cases. Thereby, for CCl_4 the Kirkwood factor decays rapidly even at high dilution to values much smaller than found in any dipolar fluid. For $CHCl_3$, which is at higher T^*, this decrease is more moderate. However, even in the latter case the need for accounting for dipole correlations is obvious.

The results pinpoint the shortcomings of the DH-based theories near criticality: The strong antiparallel correlations between neighboring dipoles reduce the dielectric constant compared with the prediction by the simpler Onsager theory. Thus, the Onsager-type expression implemented in the DHEb+DI+DD version overestimates the increase of the dielectric constant with increasing density of ion pairs, and subsequently the ionicity is largely overestimated. An implementation of the Kirkwood form (9) into the equation of state is expected to improve agreement with experiment and with Monte–Carlo data considerably, although there is then the need to model the Kirkwood factor.

ROLE OF SHORT-RANGE INTERACTIONS: AQUEOUS SOLUTIONS OF HYDROPHOBIC IONS

At the end, we briefly come to the question to what extent such corresponding-states correlations may be affected or even become obsolete due to the presence of specific interactions. Actually, Fig. 6 shows a striking influence of such effects upon the critical temperatures along a homologous series of alcohols. A similar observation has been reported by Pitzer [4]: If one adds the polyhydric alcohol 1,4-butanediol to a solution of Bu_4NPic in 1-dodecanol the good agreement of the coexistence curve with the RPM prediction deteriorates rapidly. We have ascribed this behavior to solvophobic effects of salts with large ions in solvents with high cohesive energy density [3].

Clear examples for the importance of such effects are solutions of tetraalkylammonium salts in water. At intermediate size of the cations, typically beginning with the butyl salts, these salts show closed miscibility loops [3]. With ε_S large one is at $T^* > 0.5$, and the ionic forces are not expected to cause phase separation, nor would one expect a marked population of ion pairs. In such systems, the primary force for ion aggregation is founded in the hydrophobic nature of the large alkyl groups in water which, apart from leading to close cation–cation pairs, also enforces cation–anion pairing. This cation–anion pairing increases with increasing size of both the cations and anions, contrary to what is expected from electrostatics [3]. In particular, there is a strong anion dependence in the series $F^- < Cl^- < Br^- < NO_3^- < I^- < SCN^- < ClO_4^- < Pic^-$ [3]. In biophysical chem-

istry this anion series is known as "lyotropic series" or "Hofmeister series", which governs many properties of biomolecules in solution, such as salting-out effects.

One way to account for the net short-range forces is to add a term Φ_{spec} for specific interactions to the equation of state, while due to high T^* the terms associated with ion pairing become insignificant. One possibility of large importance in practical calculations is a virial series similar to that used for gases. Because the short-range forces are screened, the virial coefficients depend now on the Debye-screening length κ [46].

A lucid example for equations of state of this type is Pitzer's ion interaction approach [47]. The thermodynamic behavior of aqueous electrolyte solutions is often described by the osmotic coefficient ϕ which in Pitzer's approach is then characterized by an expansion of the general form

$$\phi = 1 + \phi_{DH} + B(\kappa)\, C \; + \; \text{higher terms} \, . \tag{10}$$

ϕ_{DH} is the DH ion–ion contribution. The second virial coefficient $B(\kappa)$ depends on the Debye screening length κ, with $\kappa^2 \propto \rho$. At $T^* > 0.5$ the DH term ϕ_{DH} cannot cause phase separation, but we have shown [30] that a sufficiently negative second virial coefficient $B(\kappa)$ indeed causes the demixing experimentally observed in aqueous solutions of the tetraalkylammonium salts.

Formulations of this type, which are suited for data analysis over wide ranges of temperature and pressure, are available. In fact, we have shown recently by such an analysis that hydrophobic salts that are immiscible with water may unmix at high pressure [48]. An interesting example of this type is aqueous Bu_4NBr, which is a standard electrolyte in many investigations of solution behavior. This salt is highly soluble at normal pressure. From an analysis of the equation of state (10) using parameters known over some range of temperature, one predicts a miscibility gap at high pressures. This could subsequently be detected experimentally above a pressure of about 7.0 kbar, using diamond anvil cell. Figure 9 shows the critical line in the p–T plane [48].

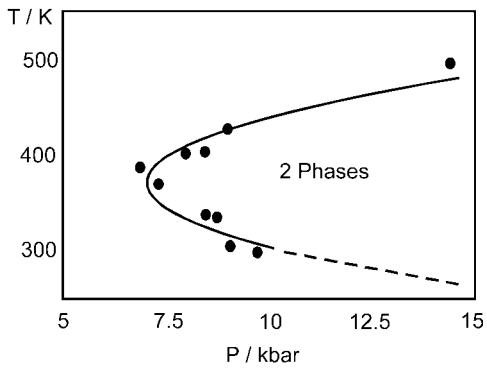

Fig. 9 High-pressure liquid–liquid immiscibility in tetra-*n*-butylammonium bromide + water. The figure shows the critical isopleth corresponding to $m \cong 2$ mol kg^{-1}.

CONCLUSIONS

Corresponding-states correlations are a useful guide for understanding equilibrium properties over wide regions of temperature, composition, and solvent dielectric constant. Much progress has been achieved in understanding the solution properties at low reduced temperatures, where specific phenomena occur. A long-known phenomenon of this type is the conductance minimum in solvents of low dielectric constant. More recently, it could be shown that liquid–liquid phase separations are also typical signatures of electrolyte behavior at low reduced temperatures. Equations of state that go beyond the simple level

of Bjerrum-type ion pair formation have been developed to describe these properties, but are not yet satisfactory in all respects. A challenge for any equation of state at low T^* is still the correct implementation of a state-dependent dielectric constant.

Unfortunately, many properties are sensitive to short-range interactions in real systems. These may render the corresponding-states analysis obsolete. In particular, the liquid–liquid critical point proves to be quite sensitive to specific interactions.

ACKNOWLEDGMENTS

I have to thank many coworkers, who, over the years, have participated in these projects. I also thank Prof. Dr. W. Schröer and Dr. V. C. Weiss from the University of Bremen for many discussions. The work was supported in parts from the Deutsche Forschungsgemeinschaft, Verband der Chemischen Industrie, and from the Alexander-von-Humboldt-Stiftung.

REFERENCES

1. H. L. Friedman and B. Larsen. *J. Chem. Phys*. **70**, 92 (1979).
2. H. Weingärtner and W. Schröer. *Adv. Chem. Phys*. **116**, 1 (2001). References cited therein.
3. H. Weingärtner, T. Merkel, U. Maurer, J.-P. Conzen, H. Glasbrenner, S. Käshammer. *Ber. Bunsenges. Phys. Chem*. **95**, 1579 (1991).
4. K. S. Pitzer. *J. Phys. Chem.* **99**, 13077 (1995). References cited therein.
5. H. Weingärtner and W. Schröer. In: *Steam, Water, and Hydrothermal Systems*, P. R. Tremaine, P. G. Hill, P. V. Balakrishnan, (Eds.), NRC Press, Ottawa (2000).
6. M. Fisher. *J. Stat. Phys*. **75**, 1 (1994). References cited therein.
7. G. Stell. *J. Stat. Phys*. **78**, 197 (1995). References cited therein.
8. H. Weingärtner, M. Kleemeier, S. Wiegand, W. Schröer. *J. Stat. Phys*. **78**, 169 (1995). References cited therein.
9. N. Bjerrum. *Kgl. Danske Vidensk. Mat.-Fys. Medd*. **7**, 1 (1926).
10. L. C. Kenausis, E. C. Evers, C. A. Kraus. *Proc. Nat. Acad. Sci. U.S.* **48**, 121 (1962).
11. K. S. Pitzer. *J. Phys. Chem*. **88**, 2689 (1984).
12. C. A. Kraus. *J. Phys. Chem*. **60**, 129 (1956).
13. R. M. Fuoss and C. A. Kraus. *J. Amer. Chem. Soc*. **55**, 2387 (1933).
14. G. Orkoulas and A. Z. Panagiotopoulos. *J. Chem. Phys*. **110**, 1582 (1999).
15. A. Z. Panagiotopoulos. *Mol. Phys*. **61**, 813 (1987).
16. B. Guillot and Y. Guissani. *Mol. Phys*. **87**, 37 (1996).
17. V. C. Weiss and W. Schröer. *J. Chem. Phys*. **108**, 7747 (1998).
18. Y. Levin and M. E. Fisher. *Physica A* **225**, 164 (1995).
19. H. Weingärtner, V. C. Weiss, W. Schröer. *J. Chem. Phys*. **113**, 762 (2000).
20. See e.g., H. Falkenhagen and W. Ebeling. In *Ionic Interactions*, S. Petrucci (Ed.), Vol. 1, Chap. VII. Academic Press, New York (1972).
21. H. Weingärtner, H. Nadolny, S. Käshammer. *J. Phys. Chem. B* **103**, 4738 (1999).
22. W. Schröer. *J. Mol. Liq.* **92**, 77 (2001).
23. H. L. Friedman. *J. Phys. Chem*. **66**, 1595 (1962).
24. E. A. S. Cavell and P. C. Knight. *Z. Phys. Chem. Neue Folge* **57**, 331 (1968).
25. W. Ebeling and M. Grigo. *Ann. Phys. (Leipzig)* **37**, 21 (1980).
26. See e.g., C. J. F. Böttcher. *Theory of Electric Polarization*, Vol. 1, Elsevier, Amsterdam, 1973.
27. See e.g., H. Fröhlich. *Theory of Dielectrics*, Clarendon, Oxford, 1959.
28. D. Laria, H. Corti, R. Fernández-Prini. *J. Chem. Soc. Faraday Trans*. **86**, 1051 (1990).
29. W. E. Price and H. Weingärtner. *J. Phys. Chem*. **95**, 8933 (1991).
30. H. Weingärtner. *Ber. Bunsenges. Phys. Chem*. **93**, 1058 (1989).

31. H. Weingärtner. Unpublished data.
32. C. H. Secoy. *J. Amer. Chem. Soc*. **72**, 3343 (1950).
33. See e.g., V. M. Valyashko. *Pure Appl. Chem*. **67**, 569 (1995).
34. V. M. Valyashko, M. A. Urusova, K. G. Kravchuk. *Dokl. Akad. Nauk SSSR* **272**, 390 (1983).
35. I. Svorstøl, H. Høyland, J. Songstad. *Acta Chem. Scand. Ser. B* **38**, 885 (1984).
36. I. Svorstøl and J. Songstad. *Acta Chem. Scand. Ser. B* **39**, 639 (1985).
37. B. Gestblom and J. Songstad. *Acta Chem. Scand. Ser. B* **41**, 396 (1987).
38. H. Nadolny, M. Ott, H. Weingärtner. Unpublished data.
39. L. C. Kenausis, E. C. Evers, C. A. Kraus. *Proc. Nat. Acad. Sci. U.S.* **49**, 141 (1963).
40. A. M. Sukhotin and Z. N. Timofeeva. *Zhur. Fiz. Khim*. **33**, 1602 (1959).
41. W. Ebeling and M. Grigo. *J. Solution Chem*. **11**, 151 (1982).
42. M. Kleemeier, S. Wiegand, W. Schröer, H. Weingärtner. *J. Chem. Phys*. **110**, 3085 (1999).
43. P. Walden and M. Centnerszwer. *Z. Phys. Chem*. **42**, 432 (1903).
44. S. Wiegand, M. Kleemeier, J. M. Schröder, W. Schröer, H. Weingärtner. *Int. J. Thermophys*. **15**, 1044 (1994).
45. H. Nadolny and H. Weingärtner. *J. Chem. Phys*. **114**, 5273 (2001).
46. J. E. Mayer. *J. Chem. Phys*. **18**, 1426 (1950).
47. K. S. Pitzer and G. Mayorga. *J. Phys. Chem*. **77**, 2300 (1973).
48. H. Weingärtner, D. Klante, G. M. Schneider. *J. Solution Chem*. **28**, 435 (1999).